Available online at www.sciencedirect.com

ScienceDirect

journal homepage: www.elsevier.com/locate/he

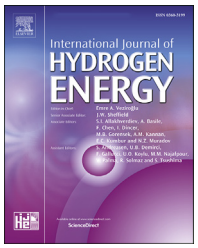

$MgTiO_3H_x$ and $CaTiO_3H_x$ perovskite compounds for hydrogen storage applications

Aysenur Gencer [a,b], *Gokhan Surucu* [a,c,d,*], *Selgin Al* [e]

[a] *Department of Physics, Middle East Technical University, Turkey*
[b] *Department of Physics, Karamanoglu Mehmetbey University, Turkey*
[c] *Department of Electric and Energy, Ahi Evran University, Turkey*
[d] *Photonics Application and Research Center, Gazi University, Turkey*
[e] *Department of Physics, Ahi Evran University, Turkey*

ARTICLE INFO

Article history:
Received 8 December 2018
Received in revised form
7 March 2019
Accepted 15 March 2019
Available online 6 April 2019

Keywords:
Perovskite materials
Hydrogen storage
First principle
Mechanical properties
Electronic properties

ABSTRACT

The first principle calculations are used to investigate hydrogen storage properties of $MgTiO_3H_x$ and $CaTiO_3H_x$ (x = 0, 3, 6, and 8) perovskite compounds in cubic phase (Pm3 m). In order to examine the stability of these compounds, formation enthalpies are calculated and all compounds (except $MgTiO_3H_6$ and $MgTiO_3H_8$) are found to be stable. The second order elastic constants and related polycrystalline elastic moduli (e.g., shear modulus, Young's modulus, Poisson's ratio, Debye temperature, sound velocities) are determined and the results are discussed in detail. The mechanical stability determination indicates that $MgTiO_3$, $CaTiO_3$, and $CaTiO_3H_6$ compounds are only stable compounds and also $MgTiO_3$ and $CaTiO_3H_6$ are ductile while $CaTiO_3$ is a brittle material. Also, the mechanical anisotropy is discussed via two-dimensional (2D) and three-dimensional (3D) surfaces for mechanical stable compounds and they are found to have anisotropic behaviour (except linear compressibility for $MgTiO_3$, $CaTiO_3$). Electronic band structure and corresponding partial density of states (PDOS) and charge density have been plotted. Bader charge analysis have been done. $MgTiO_3$ has metallic behaviour whereas $CaTiO_3$ and $CaTiO_3H_6$ have semiconductor behaviour. Among all compounds, $CaTiO_3H_6$ is found to be only one that could be used in the hydrogen storage applications. For this compound, the gravimetric hydrogen storage capacity is calculated as 4.27 wt% and the hydrogen desorption temperature is obtained as 827.1 K.

Introduction

The energy demand of today's modern society increases due to several reasons such as uprising living standards and population. This demand is mostly satisfied by use of fossil fuels according to International Energy Agency (IEA) [1] which results in production of anthropogenic CO_2 and catastrophic weather events such as flooding, deforestation and droughts. It is said that a 2 °C increase in world's temperature will threat the human existence in the world. Moreover, this fast consumption of fossil fuels will lead to depletion of resources quickly. These concerns have promoted to the search for

* *Corresponding author*. Department of Physics, Middle East Technical University, Turkey.
E-mail address: g_surucu@yahoo.com (G. Surucu).
https://doi.org/10.1016/j.ijhydene.2019.03.116

sustainable, clean, practical and environmentally favourable energy sources and carriers.

Currently, renewable energy sources (wind, solar, biomass, hydropower and wave power) seem to be the options. However, they have efficiency and fluctuation related drawbacks. One of the best options include hydrogen which attracts a great deal of attention by the researchers due to the fact that it is non-toxic, carbon free, easy to produce, and abundant in nature [2,3]. Hydrogen has higher energy content than that of gasoline by weight (3 times higher) but lower energy content by volume (4 times lower) [4]. It is proven to be much efficient (~% 60) than gasoline (~% 22) and diesel (~% 45) [5]. Hydrogen can play a significant role in transportation and portable applications as an energy carrier. In order to utilise hydrogen as an energy carrier a few factors need to be addressed; production, transportation and storage. This study will focus on new materials for storage of hydrogen.

Present hydrogen storage methods include gas, liquid and solid state hydrogen storage [4]. Among these methods, solid state storage of hydrogen such as metal or complex hydrides offers storing hydrogen with high gravimetric and volumetric densities [6–9]. Complex metal hydrides formed by light elements including boron, nitrogen or aluminium (e.g. $LiBH_4$, $NaBH_4$, $NaAlH_4$ …) have very high hydrogen density, however they suffer from poor thermodynamic and kinetic properties [10]. Also, Mg-based alloys are considered as promising materials for hydrogen storage with high gravimetric hydrogen storage capacities while having slow hydrogen desorption kinetics [11–13].

Recently, perovskite type metal hydrides (ABH_3) get attention as hydrogen storage materials owing to their high hydrogen storage capacity [1,14]. Traditionally, perovskite materials have ABX_3 structure where A and B are cations and X is an anion. The magnesium based perovskite type hydrides such as $NaMgH_3$ have taken particular interest by the researchers because of their high hydrogen storage capacity [15–17]. Also, $CaNiH_3$ type perovskite hydrides were considered for hydrogen storage [18,19] and Ikeda et al. [19] reported similar desorption features whilst the hydrogen desorption of $CaNiH_3$ was higher than that of $CaCoH_3$.

The presented solid-state hydrogen storage materials are the commonly studied material groups in the literature with having some drawbacks. However, the perovskite materials having ceramic nature and being hard materials could be a possible material candidate for the solid-state hydrogen storage method. In addition, these properties could lead to usage in portable applications. The main motivation of this study is to investigate the hydrogen storage properties of perovskite materials. But there is no study in the literature for perovskite materials and hydrogen storage except the aforementioned perovskite type hydrides. Hence, $MgTiO_3$ and $CaTiO_3$-based systems with H^+ - ion insertion are systematically investigated in the framework of Density Functional Theory (DFT) in the present work. The electronic properties, elastic properties, and hydrogen bonding characteristics are obtained and analysed. To the best of authors' knowledge, this is the first study that takes this approach into account for these kinds of perovskite materials. Thus, this study not only offers new data to the literature but also new materials and perspective for hydrogen storage.

Method of computation

Cubic $MgTiO_3$ and $CaTiO_3$ compounds have been investigated using DFT implemented in Vienna Ab-initio Simulation Package (VASP) [20,21]. The projector augmented wave (PAW) method [22,23] has been used for the electron-ion interaction with energy cut offs of 800 eV and 600 eV for $MgTiO_3$ and $CaTiO_3$, respectively. The generalized gradient approximation (GGA) with Perdew-Burke-Ernzerhof functional [24] has been employed for electron-electron interaction. Gamma centred k-points meshes have been generated with $12 \times 12 \times 12$ sampling. The well optimized structures have been obtained with an energy tolerance criterion of 10^{-9} eV per unit cell. Moreover, the Hellman-Feynman forces and stresses have been minimised with a convergence criterion of 10^{-10} eV/Å. The stress-strain method that is implemented in VASP, has been used to determine the elastic constants (C_{ij}).

Results and discussion

Structural and mechanical properties

The $MgTiO_3H_x$ and $CaTiO_3H_x$ (x = 0, 3, 6, 8) compounds are optimized in the cubic structures (Space group: 221, Pm3 m) shown in Fig. 1. The lattice constants (a), formation energies (ΔE_f), densities (ρ), and the Wyckoff positions of the atoms are presented in Table 1 along with the available literature results. The positions of H atoms at the most stable positions are determined by energy minimisation for the compounds. As can be seen from Table 1, the obtained lattice parameters of $CaTiO_3$ and $MgTiO_3$ are in well accordance with the reported results in literature [25–27]. In addition, there is no study to compare the results for the $MgTiO_3H_x$ and $CaTiO_3H_x$ compounds in the literature. When the number of H atoms increases in the structure, the lattice constant increases as expected. The formation energies of suggested compounds are also calculated using Eq. (1) which provides vital information about energetic stability of these compounds. All values of ΔE_f are negative except for $MgTiO_3H_6$ and $MgTiO_3H_8$ which mean that these compounds are stable. The positive value of ΔE_f exhibits completely unstable compounds, $MgTiO_3H_6$ and $MgTiO_3H_8$. The most negative formation energies can be ordered as $CaTiO_3$ > $CaTiO_3H_3$ > $MgTiO_3$ > $CaTiO_3H_6$ > $MgTiO_3H_3$ > $CaTiO_3H_8$ > $MgTiO_3H_6$. It is worth noting that insertion of H atoms into the structure results in more positive ΔE_f values.

$$\Delta E_f = E_t(CaTiO_3) - [E(Ca) + E(Ti) + 3{*}E(O)] \quad (1)$$

The mechanical stabilities of compounds are determined using three independent elastic constants (C_{11}, C_{12}, C_{44}) that are the necessary constants of the cubic crystal structures given in Table 2 and these constants are calculated using stress-strain method implemented in VASP. For a cubic crystal structure, the well-known Born criteria given below should be satisfied [28,29];

$$(C_{11} - C_{12}) > 0, \quad C_{11} > 0, \quad C_{44} > 0, \quad (C_{11} + 2C_{12}) > 0 \quad (2)$$

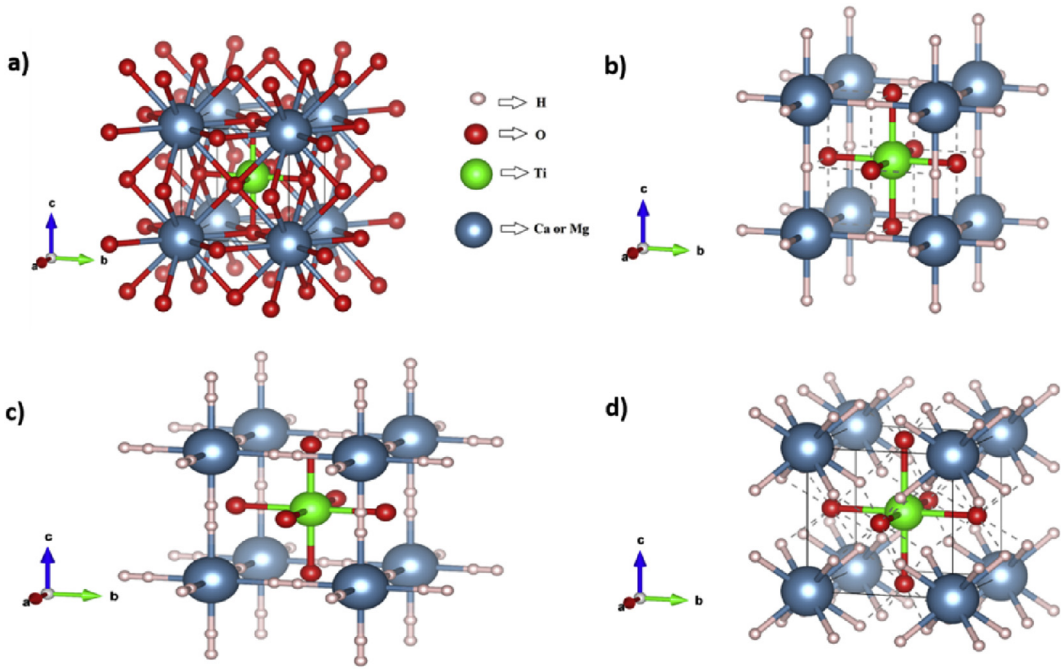

Fig. 1 – The crystal structures of a) $ATiO_3$, b) $ATiO_3H_3$, c) $ATiO_3H_6$, d) $ATiO_3H_8$ where A is Mg or Ca.

Table 1 – Lattice parameter a (Å), formation energy ΔE_f (eV/atom), density ρ (g/cm^3) and Wyckoff positions for the atoms for $MgTiO_3H_x$ and $CaTiO_3H_x$ (x = 0, 3, 6, 8).

Compounds	*a*	ΔE_f	ρ	Atomic Positions
$MgTiO_3$	3.73	−1.37	3.85	Mg: 1a (0.0, 0.0, 0.0)
	3.84 [25]			Ti: 1b (0.5, 0.5, 0.5)
				O: 3c (0.0, 0.5, 0.5)
$MgTiO_3H_3$	3.93	−0.34	3.38	H: 3d (0.0, 0.0, 0.5)
$MgTiO_3H_6$	4.31	0.08	2.63	H: 6f (0.088, 0.5, 0.5)
$MgTiO_3H_8$	4.44	0.49	2.44	H: 8g (0.267, 0.267, 0.267)
$CaTiO_3$	3.88	−4.53	3.87	Ca: 1a (0.0, 0.0, 0.0)
	3.89 [26]		3.84 [26]	Ti: 1b (0.5, 0.5, 0.5)
	3.81 [27]			O: 3c (0.0, 0.5, 0.5)
$CaTiO_3H_3$	4.07	−1.68	3.41	H: 3d (0.0, 0.0, 0.5)
$CaTiO_3H_6$	4.35	−1.12	2.86	H: 6e (0.412, 0.0, 0.0)
$CaTiO_3H_8$	4.56	−0.13	2.52	H: 8g (0.270, 0.270, 0.270)

The mechanical stability conditions also bring a restriction for bulk modulus B as follows;

$$C_{12} < B < C_{11} \quad (3)$$

Table 2 – Elastic constants C_{ij} (GPa) for $MgTiO_3H_x$ (x = 0, 3) and $CaTiO_3H_x$ (x = 0, 3, 6, 8).

Compounds	C_{11}	C_{12}	C_{44}
$MgTiO_3$	354.7	53.0	27.9
	339.0 [30]	102.0 [30]	72.0 [30]
$MgTiO_3H_3$	117.9	150.6	22.7
$CaTiO_3$	337.2	98.6	97.0
	342.1 [26]	93.3 [26]	94.5 [26]
	356.0 [30]	103.0 [30]	98.0 [30]
$CaTiO_3H_3$	53.2	183.4	14.2
$CaTiO_3H_6$	261.5	22.5	33.6
$CaTiO_3H_8$	40.9	103.3	−16.2

These parameters can give a good insight of the stability and stiffness of the compounds. As can be seen from Table 2, $MgTiO_3$, $CaTiO_3$, and $CaTiO_3H_6$, confirm the stability conditions given in Eqs. (2) and (3). Thus, it can be said that these compounds are mechanically stable in this phase. Also, the results are consistent with the available literature for $MgTiO_3$ [30] and $CaTiO_3$ [26,30]. In addition, the resistance to compression along the x-axis can also be predicted from the value of C_{11}. The order of C_{11} values for the related compounds are; $MgTiO_3$ > $CaTiO_3$ > $CaTiO_3H_6$, showing that $CaTiO_3H_6$ is the least compressible compound along the x-axis among them.

Bulk modulus (B), Shear modulus (G), Young's modulus (E), Poisson' ratio (ν), G/B and B/G ratios of the studied compounds are also obtained using calculated elastic constants as given in Table 3. In the literature, there is only one study [26] for $CaTiO_3$ to compare the obtained results here. Bulk modulus is the volume change of a material under hydrostatic pressure.

Table 3 – Bulk modulus B (GPa), shear modulus G (GPa), Young's modulus E (GPa), Poisson's ratio ν, G/B ratio and B/G ratio for $MgTiO_3$ and $CaTiO_3H_x$ (x = 0, 6).

Compounds	B	G	E	ν	G/B	B/G
$MgTiO_3$	153.5	59.1	157.1	0.329	0.385	2.597
$CaTiO_3$	178.1	105.3	263.8	0.253	0.591	1.692
	176.2 [26]	105.5 [26]	263.8 [26]	0.250 [26]	0.599 [26]	1.670 [26]
$CaTiO_3H_6$	102.1	57.5	145.2	0.263	0.563	1.776

Shear modulus is defined as the material's resistance to shape change at constant volume. Young's Modulus is the ratio of tensile stress to tensile strain. It provides information about stiffness of a material. In other words, higher *E* means, stiffer material. As can be deduced from Table 3, $CaTiO_3$ has the highest bulk modulus, shear modulus and Young's modulus among the studied materials and also obtained results are consistent with the available literature result [26]. Also, when the hydrogen bonded to $CaTiO_3$, the bulk modulus, shear modulus and Young's modulus decrease. This means that $CaTiO_3H_6$ is less stiffness and more volume change with pressure. The bulk modulus is higher than the shear modulus for these compounds that indicate the easiness of the shear deformation than compressional deformation. Moreover, the obtained results could be compared with the most studied perovskite type hydride $NaMgH_3$ [16] and it is deduced that $CaTiO_3H_6$ has higher bulk modulus, shear modulus and Young's modulus than $NaMgH_3$. So, $CaTiO_3H_6$ is more stiffness and is hard to deform with shear deformation and compressional deformation. In addition, Poisson's ratios of compounds are determined. Poisson's ratio can be used to predict bonding properties of a material and it is defined as the measure of the expansion of perpendicular directions to the direction of compression or the measure of contraction of perpendicular directions to the direction of stretching. Poisson's ratio is suggested as 0.1 for covalent materials and 0.25 for ionic materials in the literature [31]. The values of Poisson's ratio for the studied compounds are above 0.25 which indicates that ionic character is dominant in all compounds. In addition, G/B ratio also called Pugh's modulus could be also used to determine the bonding nature of a material. If G/B ratio is around 1.1, the material has dominantly covalent bonding if it is around 0.6, the ionic bonding is dominant [32]. All compounds have G/B ratio around 0.6 as can be seen from Table 3, these materials have dominantly ionic bonding consistent with the result of the Poisson's ratio. Further investigations are carried out by examining the ratio of bulk modulus to shear modulus (*B/G*). This ratio is an indication of the material's ductility or brittleness. According to Pugh [33] if *B/G* is higher than 1.75, the material is ductile otherwise it is brittle. Based on this criterion and the obtained values given in Table 3, it is seen that $MgTiO_3$ and $CaTiO_3H_6$ are ductile whereas $CaTiO_3$ is a brittle material. For hydrogen storage applications, the ductile materials are preferable because they do not need any requirements. However, the brittle materials could require to extra caution to keep the material in safe especially for a portable application. So, $CaTiO_3H_6$ is a preferable material for hydrogen storage applications.

The anisotropic elastic properties have been studied using ELATE program [34]. The calculated elastic constants are employed to program to obtain two-dimensional (2D) and three-dimensional (3D) changes in linear compressibility (β), Shear modulus, Young's modulus and Poisson's ratio. Here only results for $CaTiO_3H_6$ are presented in Fig. 2 due to save space in the journal. In addition, the maximum and minimum values for related parameters for the studied compounds are given in Table 4. It is known that if a material is isotropic, the shapes resemble to a spherical shape, deviation from isotropy results in a deviation from the spherical shape. The maximum values for the parameters are shown with green curves or spheres while the minimum ones are shown with blue curves or spheres. Fig. 2 and Table 4 clearly illustrate that Shear modulus, Young's modulus and Poisson's ratio of $CaTiO_3H_6$ have anisotropic behaviour whereas the linear compressibility of $CaTiO_3H_6$ show isotropic behaviour.

Debye temperature (Θ_D) is one of the important physical parameters of a material which provides information about various properties such as melting temperature, elastic stiffness and specific heat. Debye temperatures of compounds are calculated using the average sound velocity (V_m), the longitudinal (V_l) and the transverse (V_t) sound velocities. The details of computation are given in Ref. [35]. The results of Debye temperatures and velocities for the compounds are given in Table 5. The orders of Debye temperatures of compounds are; $CaTiO_3H_6 > CaTiO_3 > MgTiO_3 > MgTiO_3H_6$. The thermal conductivities of compounds are also computed using two different theoretical models; Clarke [36,37] and Cahill [38]. Both models provide lower limit of the thermal conductivity (λ_{min}) which are presented in Table 5 along with average mass per atom (M_a) for Clarke model and the density of number of atoms per volume (*n*) for Cahill model. Table 5 point outs that the thermal conductivity of $CaTiO_3$ increases with the addition of hydrogen to the cubic structures.

Electronic properties

The structural and mechanical properties investigation reveals that only three compounds ($MgTiO_3$, $CaTiO_3$ and $CaTiO_3H_6$) are both energetically and mechanically stable.

The band structures for $MgTiO_3$, $CaTiO_3$, and $CaTiO_3H_6$ are predicted along the high symmetry directions in the first Brillouin zone from the calculated equilibrium lattice constant. It is found that $MgTiO_3$ has metallic character while $CaTiO_3$ (with the indirect band gap value of 1.89 eV) and $CaTiO_3H_6$ (with the indirect band gap value of 1.23 eV) have semiconductor behaviour. Due to the main focus of the study is hydrogen storage, the band structures and corresponding total density of state (TDOS) are displayed only for $CaTiO_3H_6$ in Fig. 3.

Furthermore, the partial density of states (PDOS) for $CaTiO_3$ and $CaTiO_3H_6$ are given in Fig. 4 to discuss the partial density of states after the hydrogen bonding to the structure. Hereby,

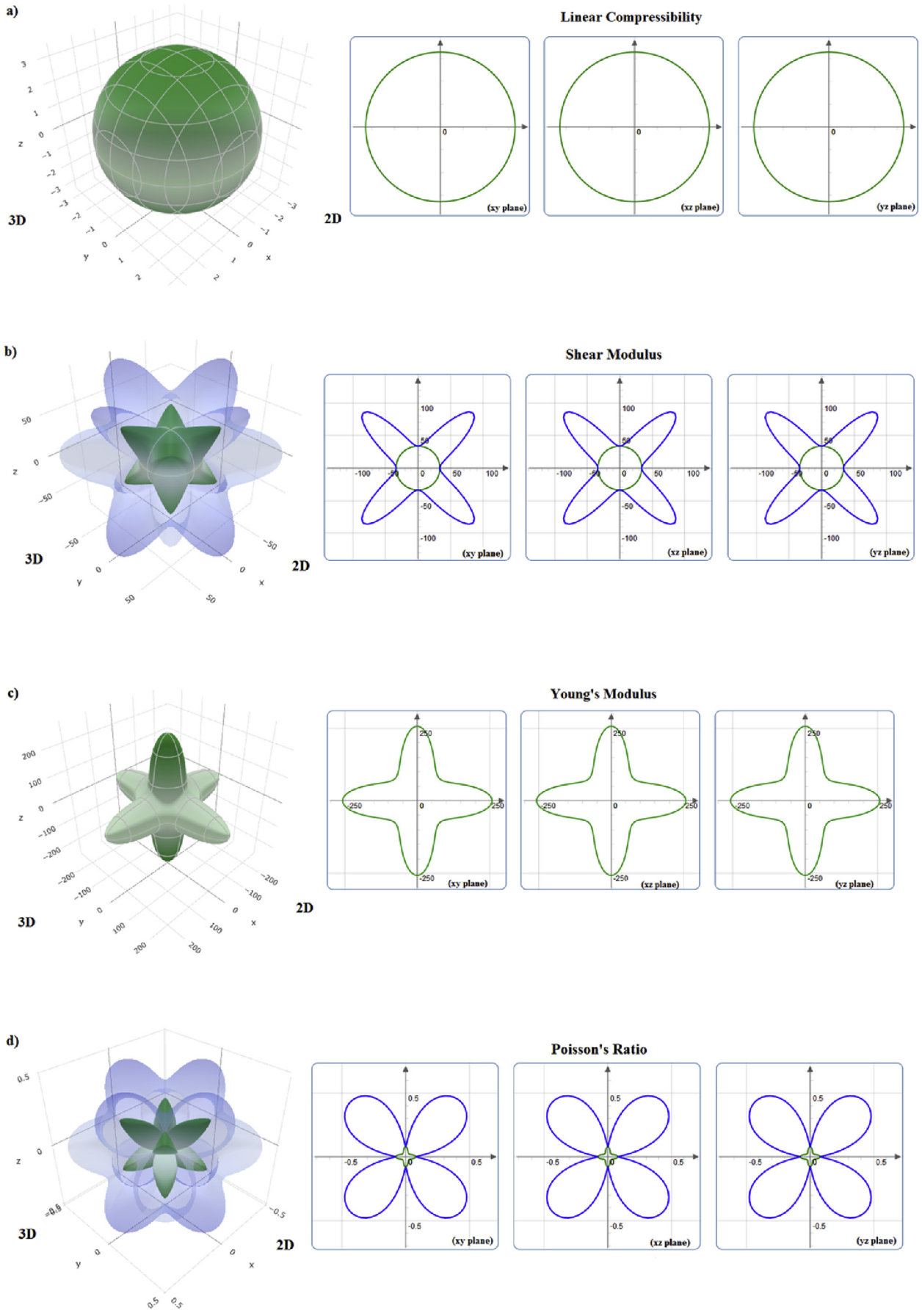

Fig. 2 – The directional dependent (a) linear compressibility, (b) Shear modulus, (c) Young's modulus and (d) Poisson's ratio of $CaTiO_3H_6$ in 3D and 2D.

Table 4 – The maximum and minimum values of the Young's modulus E (GPa), linear compressibility β (TPa^{-1}), shear modulus G (GPa) and Poisson's ratio ν of $MgTiO_3$ and $CaTiO_3H_x$ (x = 0, 6).

Compounds	E (GPa)		β (TPa^{-1})		G (GPa)		ν	
	E_{min}	E_{max}	β_{min}	β_{max}	G_{min}	G_{max}	ν_{min}	ν_{max}
$MgTiO_3$	78.92	340.92	2.17	2.17	27.90	150.85	0.04	0.75
$CaTiO_3$	246.29	292.58	1.87	1.87	97.00	119.30	0.19	0.32
$CaTiO_3H_6$	90.83	257.93	3.26	3.27	33.60	119.37	0.03	0.61

Table 5 – Debye temperature (Θ_D in K), longitudinal (V_l in m/s), transverse (V_l in m/s) and average wave velocities (V_m in m/s), minimum thermal conductivities (λ_{min} in $W_m^{-1}K^{-1}$) average mass per atom (M_a) for Clarke model and the density of number of atoms per volume (n) for Cahill model for $MgTiO_3$ and $CaTiO_3H_x$ (x = 0, 6) compounds.

Compounds	Θ_D	V_l	V_t	V_m	Clarke model		Cahill model	
					M_a (10^{-26})	λ_{min}	n (10^{28})	λ_{min}
$MgTiO_3$	599.6	7763	3915	4390	3.991	1.614	9.600	1.827
$CaTiO_3$	760.2	9067	5213	5790	4.515	1.928	8.500	2.111
$CaTiO_3H_6$	771.8	8082	4561	5073	2.143	2.235	13.300	2.453

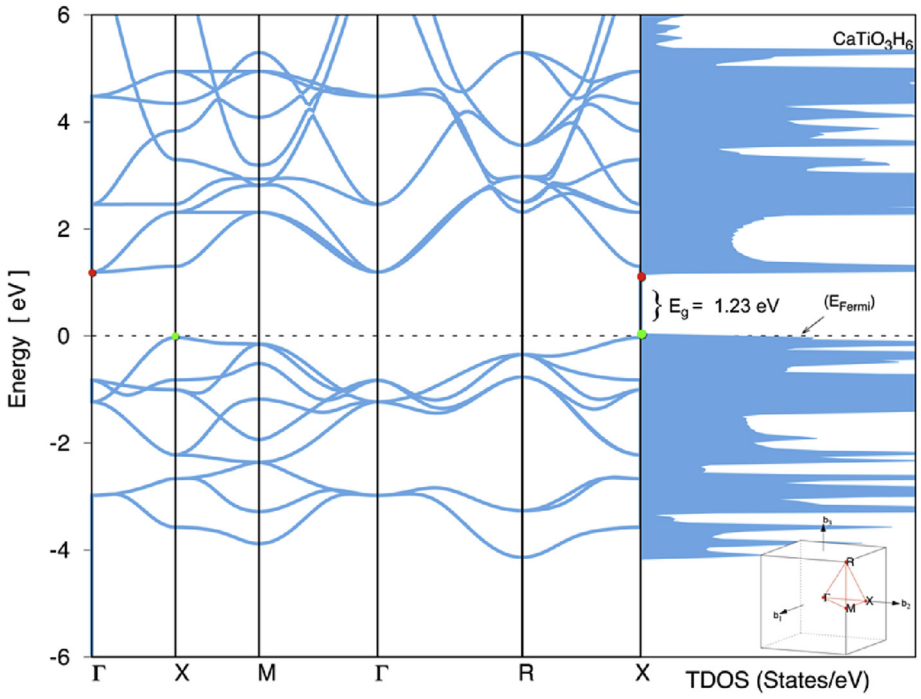

Fig. 3 – Calculated partial and total density of states of $CaTiO_3H_6$.

the bonding character demonstrated by the PDOS gives information on hybridization and the orbital character of the states. The most contribution comes from the p states of O below the Fermi level for both compounds. The most contribution above the Fermi level comes from d states of Ti for $CaTiO_3$ while it comes from d states of Ti, p states of Ca and O for $CaTiO_3H_6$.

The charge densities for these compounds have been obtained and only the result for $CaTiO_3H_6$ is given in Fig. 5. As can be seen from the figure, $CaTiO_3H_6$ has ionic bonding which is consistent with the result from the Poisson's ratio and G/B ratio.

In order to determine the charge of each ion in the compounds, Bader partial charge analysis have been carried out and the results are given in Table 6. The Bader charges are computed using VASP code and the results are analysed using algorithm developed by Henkelman et al. [39]. Which is based on Bader's approach [40]. In Table 6, positive charge represents charge transfer from the atom whereas negative charge means charge transfer to the atom [41]. Ca or Mg atoms and Ti atoms give away charges while O and H atoms get charges as can be concluded from Table 6. For $CaTiO_3H_6$, the charges are transferred away from Ca and Ti atoms while these charges transferred to O and H atoms.

Hydrogen storage properties

$CaTiO_3H_6$ is the only stable compound both energetically and mechanically. Therefore, hydrogen storage properties are

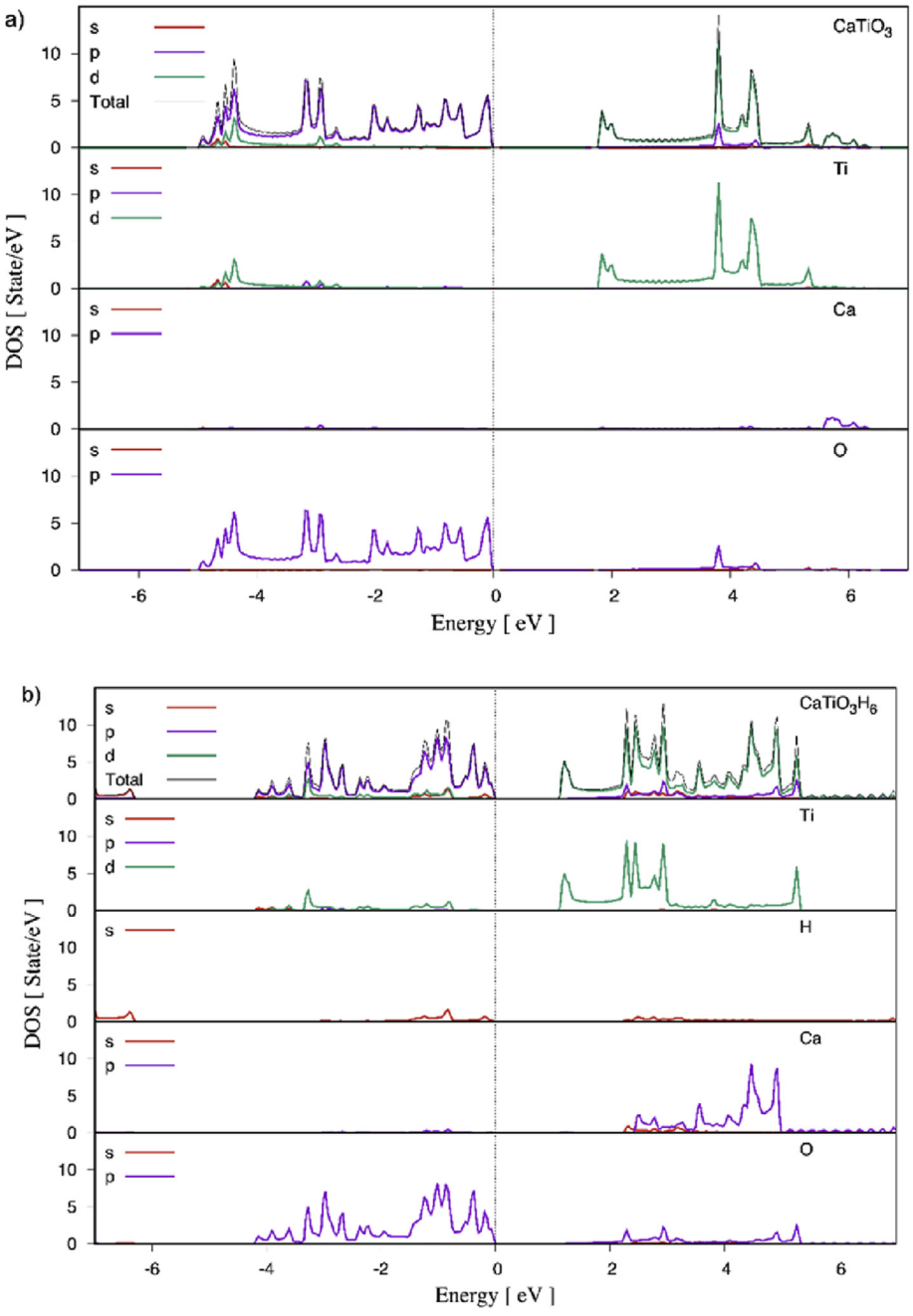

Fig. 4 – Partial density of states for (a) $CaTiO_3$ and (b) $CaTiO_3H_6$.

investigated for it. The gravimetric hydrogen storage capacity ($C_{wt\%}$) is an important parameter for hydrogen storage applications that is the amount of hydrogen stored per unit mass of a material. Therefore, determination of it is essential for the applications. The gravimetric hydrogen storage capacity could be calculated using Eq. (4) [42] where H/M is the hydrogen to material atom ratio, M_H is the molar mass of H and M_{Host} is the molar mass of the host material. The gravimetric hydrogen storage capacity of $CaTiO_3H_6$ is calculated as 4.27 wt%.

$$C_{wt\%} = \left(\frac{\left(\frac{H}{M}\right) M_H}{M_{Host} + \left(\frac{H}{M}\right) M_H} \times 100 \right) \% \quad (4)$$

In addition to the gravimetric hydrogen storage capacity, the hydrogen desorption temperature (T) should be obtained in order to consider its usage in applications. The hydrogen desorption temperature is the required temperature to release H from the structure and could be calculated using Eq. (5) where ΔH is the calculated formation enthalpy and ΔS is the entropy change of H which is 130.7 J/mol.K [43]. The hydrogen desorption temperature of $CaTiO_3H_6$ is obtained as 827.1 K.

$$\Delta H = T \times \Delta S \quad (5)$$

The $CaTiO_3H_6$ compound is hypothetical therefore there is no experimental data nor theoretical study in order to compare the calculation results. However, the perovskite type

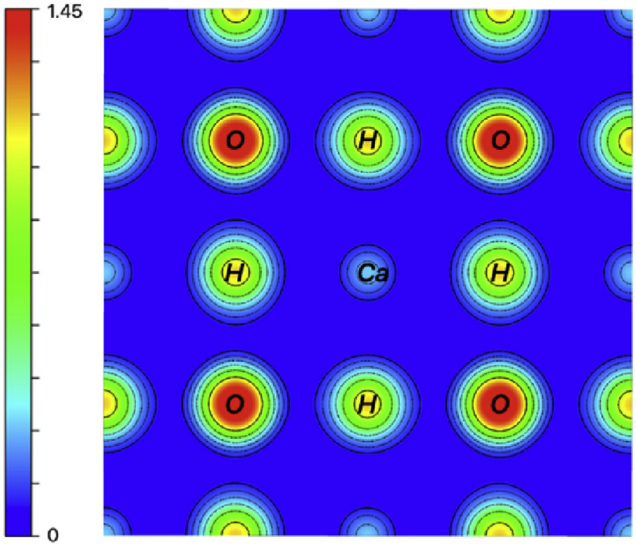

Fig. 5 – Charge density of $CaTiO_3H_6$.

Table 6 – Total Bader partial charge for the ions of $MgTiO_3$ and $CaTiO_3H_x$ (x = 0 and 6) in units of e.

Ion	$MgTiO_3$	$CaTiO_3$	$CaTiO_3H_6$
Mg/Ca	1.873	1.587	1.430
Ti	2.116	2.075	2.059
O	−3.989	−3.662	−3.456
H	x	x	−0.033

hydrides [44–47] could be used to compare the obtained results. Therefore, $CaNiH_3$ [19] has been chosen from the literature for the comparison. It has been measured that $CaNiH_3$ releases an amount of 1.0 wt% H below 650 K and the total hydrogen storage capacity has been determined 2.9 wt% with hydrogen analysis [19]. So, $CaTiO_3H_6$ has more gravimetric storage capacity than $CaNiH_3$. The hydrogen desorption for releasing one third of hydrogen stored in $CaNiH_3$ is below 650 K while the hydrogen desorption temperature of $CaTiO_3H_6$ is 827.1 K to release the full amount of the stored hydrogen. So, $CaTiO_3H_6$ has more gravimetric storage capacity and low hydrogen desorption temperature than $CaNiH_3$.

Conclusion

This study focuses on searching new materials and revealing their physical properties for solid state hydrogen storage. This type of research is crucial to promote usage of hydrogen technology especially for on-board applications. In this sense, $MgTiO_3$ and $CaTiO_3$ perovskite compounds are investigated for hydrogen storage in terms of structural, mechanical, electronic and hydrogen storage properties systematically by using first principle calculations. The cubic $MgTiO_3$ and $CaTiO_3$ structures have been optimized and then hydrogen bonding to optimized structures have been performed. Then, the properties of these suggested compounds are studied and it has been found that $MgTiO_3H_6$ and $MgTiO_3H_8$ are unstable compounds. The mechanical stability investigation of the energetically stable compounds reveal that only $MgTiO_3$, $CaTiO_3$ and $CaTiO_3H_6$ compounds are both energetically and mechanically stable compounds. All compounds have ionic bonding and also, $MgTiO_3$ and $CaTiO_3H_6$ are ductile whereas $CaTiO_3$ is brittle. The directional anisotropy calculations of compounds suggest that shear modulus, Young's modulus and Poisson's ratio of all compounds have anisotropic behaviour except for the linear compressibility which shows isotropic behaviour. The electronic band structures of the compounds show that $CaTiO_3$ and $CaTiO_3H_6$ has band gaps as 1.89 eV and 1.23 eV, respectively. The Bader partial charge analysis shows that the charges are transferred away from Mg/Ca and Ti atoms while these charges transferred to O and H atoms. Moreover, the gravimetric hydrogen storage capacity of $CaTiO_3H_6$ is calculated as 4.27 wt% and the hydrogen desorption temperature is determined as 827.1 K. These properties are important for hydrogen storage applications. This work is the first known study for $MgTiO_3H_x$ and $CaTiO_3H_x$ perovskite compounds and their hydrogen storage application that provides some insights for the future theoretical and experimental studies.

Author contributions

Conceived the study: A. G. (50%), G. S. (45%) and S. A. (5%); wrote the paper: A. G. (50%), G. S. (45%) and S. A. (5%).

Acknowledgments

This work was supported by the Ahi Evran University Research Project Unit under Project No PYO-KMY.4001.15.001.

REFERENCES

[1] International Energy Agency. Global Energy and CO_2 Status Report, the latest trends in energy and emissions in. 2017. https://www.iea.org/geco/. [Accessed 29 November 2018].
[2] Sreedhar I, et al. A Bird's Eye view on process and engineering aspects of hydrogen storage. Renew Sustain Energy Rev 2018;91:838–60. https://doi.org/10.1016/j.rser.2018.04.028.
[3] Dutta S. A review on production, storage of hydrogen and its utilization as an energy resource. J Ind Eng Chem 2014;20(4):1148–56. https://doi.org/10.1016/j.jiec.2013.07.037.
[4] Züttel A. Hydrogen storage methods. Naturwissenschaften 2004;91:157–72. https://doi.org/10.1007/s00114-004-0516-x.
[5] Hirose K. Handbook of hydrogen storage: new materials for future energy storage. John Wiley & Sons; 2010.
[6] Sakintuna B, Lamari-Darkrim F, Hirscher M. Metal hydride materials for solid hydrogen storage: a review. Int J Hydrogen Energy 2007;32(9):1121–40. https://doi.org/10.1016/j.ijhydene.2006.11.022.
[7] Jena P. Materials for hydrogen storage: past, present, and future. J Phys Chem Lett 2011;2(3):206–11. https://doi.org/10.1021/jz1015372.
[8] Chen P, Zhu M. Recent progress in hydrogen storage. Mater Today 2008;11(12):36–43. https://doi.org/10.1016/S1369-7021(08)70251-7.
[9] Orimo SI, et al. Complex hydrides for hydrogen storage. Chem Rev 2007;107(10):4111–32. https://doi.org/10.1021/cr0501846.
[10] Moller KT, et al. Complex metal hydrides for hydrogen, thermal and electrochemical energy storage.

Energies 2017;10(10):30. https://doi.org/10.3390/en10101645.
[11] Zhu M, Wang H, Ouyang LZ, Zeng MQ. Composite structure and hydrogen storage properties in Mg-base alloys. Int J Hydrogen Energy 2006;31:251–7. https://doi.org/10.1016/j.ijhydene.2005.04.030.
[12] Jain IP, Lal C, Jain A. Hydrogen storage in Mg: a most promising material. Int J Hydrogen Energy 2010;35:5133–44. https://doi.org/10.1016/j.ijhydene.2009.08.088.
[13] Baysal MB, Surucu G, Deligoz E, Ozısık H. The effect of hydrogen on the electronic, mechanical and phonon properties of LaMgNi4 and its hydrides for hydrogen storage applications. Int J Hydrogen Energy 2018;43(52):23397–408. https://doi.org/10.1016/j.ijhydene.2018.10.183.
[14] Ikeda K, et al. Formation region and hydrogen storage abilities of perovskite-type hydrides. Prog Solid State Chem 2007;35(2–4):329–37. https://doi.org/10.1016/j.progsolidstchem.2007.01.005.
[15] Pottmaier D, et al. Structure and thermodynamic properties of the $NaMgH_3$ perovskite: a comprehensive study. Chem Mater 2011;23(9):2317–26. https://doi.org/10.1021/cm103204p.
[16] Bouhadda Y, Bououdina M, Fenineche N, Boudouma Y. Elastic properties of perovskite-type hydride $NaMgH_3$ for hydrogen storage. Int J Hydrogen Energy 2013;38(3):1484–9. https://doi.org/10.1016/j.ijhydene.2012.11.047.
[17] Reshak AH. $NaMgH_3$ a perovskite-type hydride as advanced hydrogen storage systems: electronic structure features. Int J Hydrogen Energy 2015;40(46):16383–90. https://doi.org/10.1016/j.ijhydene.2015.10.030.
[18] Sato T, et al. Hydrides with the perovskite structure: general bonding and stability considerations and the new representative $CaNiH_3$. J Solid State Chem 2005;178(11):3381–8. https://doi.org/10.1016/j.jssc.2005.08.026.
[19] Ikeda K, et al. Formation of perovskite-type hydrides and thermal desorption processes in Ca–T–H (T=3d transition metals). Scripta Mater 2006;55(9):827–30. https://doi.org/10.1016/j.scriptamat.2006.07.016.
[20] Kresse G, Furthmüller J. Efficient iterative schemes for ab initio total-energy calculations using a plane-wave basis set. Phys Rev B 1996;54(16):11169. https://doi.org/10.1103/PhysRevB.54.11169.
[21] Kresse G, Furthmüller J. Efficiency of ab-initio total energy calculations for metals and semiconductors using a plane-wave basis set. Comput Mater Sci 1996;6(1):15–50. https://doi.org/10.1016/0927-0256(96)00008-0.
[22] Kresse G, Joubert D. From ultrasoft pseudopotentials to the projector augmented-wave method. Phys Rev B 1999;59(3):1758. https://doi.org/10.1103/PhysRevB.59.1758.
[23] Blöchl PE. Projector augmented-wave method. Phys Rev B 1994;50(24):17953. https://doi.org/10.1103/PhysRevB.50.17953.
[24] Perdew JP, Burke K, Ernzerhof M. Generalized gradient approximation made simple. Phys Rev Lett 1996;77(18):3865. https://doi.org/10.1103/PhysRevLett.77.3865.
[25] Pandech N. Master thesis. Suranaree University of Technology; 2013.
[26] Tariq S, et al. Structural, electronic and elastic properties of the cubic $CaTiO_3$ under pressure: a DFT study. AIP Adv 2015;5(7). 077111, https://doi.org/10.1063/1.4926437.
[27] Moriwake H, et al. First-principles calculations of lattice dynamics in $CdTiO_3$ and $CaTiO_3$: phase stability and ferroelectricity. Phys Rev B 2011;84(10):104114. https://doi.org/10.1103/PhysRevB.84.104114.
[28] Wu Z, Zhao E, Xiang H, Hao X, Liu X, Meng J. Crystal structures and elastic properties of superhard IrN_2 and IrN_3 from first principles. Phys Rev B 2007;76:054115. https://doi.org/10.1103/PhysRevB.76.054115.
[29] Born M. On the stability of crystal lattices. I. Math Proc Cambridge Philos Soc 1940;36:160. https://doi.org/10.1017/S0305004100017138.
[30] Pandech N, Sarasamak K, Limpijumnong S. Elastic properties of perovskite $ATiO_3$ (A = Be, Mg, Ca, Sr, and Ba) and $PbBO_3$ (B = Ti, Zr, and Hf): first principles calculations. J Appl Phys 2015;117:1–5. 174108, https://doi.org/10.1063/1.4919837.
[31] Bannikov VV, Shein IR, Ivanovskii AL. Electronic structure, chemical bonding and elastic properties of the first thorium-containing nitride perovskite $TaThN_3$. Phys Status Solidi Rapid Res Lett 2007;1(3):89–91. https://doi.org/10.1002/pssr.200600116.
[32] Gencer A, Surucu G. Electronic and lattice dynamical properties of Ti_2SiB MAX phase. Mater Res Express 2018;5(076303):1–9. https://doi.org/10.1088/2053-1591/aace7f.
[33] Pugh SF. *XCII*. Relations between the elastic moduli and the plastic properties of polycrystalline pure metals. Philos Mag J Sci 1954;45(367):823–43. https://doi.org/10.1080/14786440808520496.
[34] Galliac R, Pullumbi P, Coudert F-X. ELATE: an open-source online application for analysis and visualization of elastic tensors. J Phys Condens Matter 2016;28:1–5. 275201, https://doi.org/10.1088/0953-8984/28/27/275201.
[35] Ozisik HB, Colakoglu K, Surucu G, Ozisik H. Structural and lattice dynamical properties of Zintl NaIn and NaTl compounds. Comput Mater Sci 2011;50:1070–6. https://doi.org/10.1016/j.commatsci.2010.11.003.
[36] Clarke DR. Materials selection guidelines for low thermal conductivity thermal barrier coatings. Surf Coating Technol 2003;163–164:67–74. https://doi.org/10.1016/S0257-8972(02)00593-5.
[37] Clarke DR, Levi CG. Materials design for the next generation thermal barrier coatings. Annu Rev Mater Res 2003;33:383–417. https://doi.org/10.1146/annurev.matsci.33.011403.113718.
[38] Cahill DG, Watson SK, Pohl RO. Lower limit to the thermal conductivity of disordered crystals. Phys Rev B 1992;46:6131–40. https://doi.org/10.1103/PhysRevB.46.6131.
[39] Henkelman G, Arnaldsson A, Jónsson H. A fast and robust algorithm for Bader decomposition of charge density. Comput Mater Sci 2006;36(3):354–60. https://doi.org/10.1016/j.commatsci.2005.04.010.
[40] Bader RFW. Atoms in molecules : a quantum theory. Oxford: Clarendon); 1990.
[41] Pan R-K, et al. First principles study on elastic and electronic properties of bialkali alanates $M_2M'AlH_6$. Int J Hydrogen Energy 2018;43(7):3862–70. https://doi.org/10.1016/j.ijhydene.2018.01.006.
[42] Broom DP. Hydrogen storage materials : the characterisation of their storage properties. Springer; 2011.
[43] Zeng Q, Su K, Zhang L, Xu Y, Cheng L, Yan X, et al. Evaluation of the thermodynamic data of CH_3SiCl_3 based on quantum chemistry calculations. J Phys Chem Ref Data 2006;35:1385–90. https://doi.org/10.1063/1.2201867.
[44] Li Y, Mi Y, Chung JS, Kang SG. First-principles studies of $K_{1-x}M_xMgH_3$ (M = Li, Na, Rb, or Cs) perovskite hydrides for hydrogen storage. Int J Hydrogen Energy 2018;43(4):2232–6. https://doi.org/10.1016/j.ijhydene.2017.10.175.
[45] Rehmat B, Rafiq MA, Javed Y, Irshad Z, Ahmed N, Mirza SM. Elastic properties of perovskite-type hydrides $LiBeH_3$ and $NaBeH_3$ for hydrogen storage. Int J Hydrogen Energy 2017;42(15):10038–46. https://doi.org/10.1016/j.ijhydene.2017.01.109.
[46] Tao S, Wang Z, Wan Z, Deng J, Zhou H, Yao Q. Enhancing the dehydriding properties of perovskite-type $NaMgH_3$ by introducing potassium as dopant. Int J Hydrogen Energy 2017;42(6):3716–22. https://doi.org/10.1016/j.ijhydene.2016.07.174.
[47] Hamioud F, Mubarak AA. Structural, elastic and optoelectronic properties of the hydrogen based perovskite compounds: ab-initio study Chinese. J Phys 2018;56(1):1–9. https://doi.org/10.1016/j.cjph.2017.11.021.